

Experimental research on instability fault of high-speed aerostatic bearing-rotor system

Dongjiang Han¹, Changliang Tang², Jinfu Yang³, Long Hao⁴

Institute of Engineering Thermophysics, Chinese Academy of Sciences, Beijing, China

¹Corresponding author

E-mail: ¹handongjiang@iet.cn, ²tangcl@iet.cn, ³yangjinfu@iet.cn, ⁴haolong@iet.cn

(Accepted 16 August 2014)

Abstract. The experimental research on high-speed aerostatic bearing-rotor system with one compressor, one turbine and coaxial four discs was developed. The gas bearing-rotor system stability under different bearing supply pressure plans was studied by experiments. The paper also presents fault features of gas film whip instability, power frequency rubbing and low frequency rubbing, which provides experimental data for gas bearing-rotor system stability study.

Keywords: aerostatic bearing, gas film whip, stability, rubbing.

1. Introduction

Gas bearings have obvious advantages of low viscosity lubricant media, low friction, low power, high precision and a long life. It is widely used in civilian and national defense applications, including precision instruments, medical devices, high-speed power units, such as ultra-precision machining field including ultra-precise spindle [1] and high speed motorized spindle, cryogenic industries including railway air conditioners and air refrigerator in aircraft environment control system [2], auxiliary power units and distributed generation field [3] including high-speed PM machine, turbochargers, micro-turbine [4]. The huge demands in these fields draw more and more researchers' attentions on characteristic studies of gas bearing and gas bearing-rotor system. The stability research of gas bearing-rotor system is one of most important contents. To adopt increasing bearing supply gas pressure for controlling power frequency vibration amplitude and stability draws many attentions in the aerostatic/hybrid gas bearing-rotor system.

San Andrés and Ryu [5] introduced a simple strategy that employs an inexpensive air pressure regulator. This regulator controls the supply pressure into the hybrid bearings to reduce or eliminate the high amplitudes of rotor motion while crossing the system critical speeds. Morosi [6] presents a detailed mathematical model for hybrid lubrication of a compressible fluid-film journal bearing, and build a multibody dynamics model of a global system comprised of rotor and hybrid journal bearing to study the lateral dynamics of the system by Campbell diagrams and stability maps. They explore the feasibility of applying active lubrication to gas journal bearings by mechatronic system with the pneumatic and dynamic characteristics of a piezoelectric actuated valve system [7], and carry experimental investigations out to validate the proof-of-concept of applying active lubrication to gas bearings. Chen [8] carried out the experimental studies in 150 Nm³/h oxygen plant. They provided the methods of increasing stability by rubber O-ring and tangential air supply. The static and dynamic characteristics of bearing were studied. By employing numerical and experimental methods, the coupling dynamics of high speed hybrid gas bearing rotor system were studied by combining with nonlinear dynamic theoretical method. This offers the reference basis and effective theoretical method for the rotor bearing system design of high speed rotating machinery. Yang Jinfu et al. [9, 10] proposed a criterion for evaluation stability of journal bearings-rotor system, and presented oil film whirling and whipping by experimental methods. Chen Ce [11] carried out a dynamic stability experiment on hydrostatic-dynamic hybrid gas lubrication bearings. The results show the effective vibration control and enhanced stability could be achieved based on the property for boundness of chaos vibration.

In summary, the research methods on bearing-rotor system stability are from linearity to nonlinearity. The research results are prominent. Most of the re-search results are based on numerical simulation. The corresponding theoretical analysis and experimental studies, especially

the stability research of high-speed gas bearing-rotor system for high-speed micro-power devices are less. To search feasible measures and methods for improving the gas bearing-rotor system stability is very necessary for engineering practices. The paper carries out the experimental investigation on characteristics of gas film whipping and rubbing in high-speed gas bearing-rotor system test bed. Nonlinear vibration analytical methods included bifurcation, spectral analysis and three-dimensional spectrum are adopted to study occurrence mechanism of gas film whipping and the effect of bearing gas supply pressure on gas film whipping. Dynamic characteristic maps of gas film whipping and rubbing are presented by experimental methods, which provides data support for identify and diagnosis of the corresponding fault.

2. Experimental facility

The experimental system includes high-pressure gas source, vibration signal testing and analyzing system, control system for bearing gas and main pipe gas pressure supply, and gas bearing-multi disc-rotor system, as shown in Fig. 1.

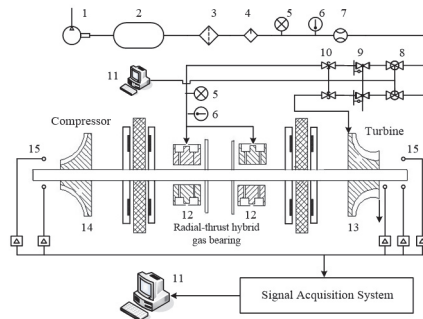


Fig. 1. Structure of experimental system: 1. Air compressor, 2. Gas tank, 3. Filter, 4. Dryer, 5. Pressure gauge, 6. Thermometer, 7. Flow meter, 8. Pressure stabilizing valve, 9. Electro-pneumatic air regulator, 10. Safety shut-off valves, 11. Computer, 12. Radial-thrust hybrid gas bearing, 13. Turbine, 14. Compressor data acquisition, 15. Eddy current displacement sensor

Table 1. Structure parameters for gas bearing-rotor system

| Geometric parameters | Symbol / Unit | Values |
|--------------------------------|---------------|--------|
| Bearing length | L / mm | 37.5 |
| Bearing inner diameter | D / mm | 25 |
| Supply hole number for one row | — | 16 |
| Bearing span | L_1 / mm | 112.75 |
| Rotor axial length | L_2 / mm | 372.24 |
| Rotor mass | M_1 / kg | 2.49 |
| Disc mass | M_2 / kg | 0.31 |
| Inside disc span | L_3 / mm | 169.70 |
| Outside disc span | L_4 / mm | 195.28 |

The control system for bearing gas and main pipe gas pressure supply is composed of the main controlled valves, regulator valves, flow meters, thermometers, manometers and gas pipelines. High pressure air provides bearing gas supply and drives radial turbine. Vibration signal testing and analyzing system is made up of eddy current displacement transducers, data-acquisition instrument, and data storage device. Three eddy current displacement transducers are placed at the turbine end for measuring vibration displacement and rotate speed. Two eddy current displacement transducers are placed at the compressor end for measuring vibration displacement.

Gas bearing-rotor system with multi discs is stated as above in Fig. 1. Rotor structure with compressor, turbine and coaxial discs is supported by two aerostatic bearings. The structural parameters of bearing-rotor system are listed as Table 1.

3. Dynamic characteristic experiments for gas bearing-rotor system with multi discs

3.1. The scheme of bearing supply gas pressure

The bearing supply gas pressure of turbine and compressor end is at 0.65 MPa from 0 r/min to 39000 rpm. The bearing supply gas pressure at the two ends increases from 0.65 MPa to 0.80 MPa when the speed arrives at 39000 r/min.

3.2. The analysis of experimental results

As the spectrum characteristic at each measured direction was similar, the analysis of vibration feature at the vertical direction of the turbine end was narrated in the following.

In the speed-up process, the highest speed is at 49615 rpm and the speed-up process is divided into 5 regions, i.e. BC region of speed soaring process, AB, CD and EF regions of sub-synchronous frequency process and M region of rubbing process. Several staircase shaped inflection points, such as 1, 2, and 3 reflect the turbine flow increasing points in the speed-up process, as shown in Fig. 2 (many similar inflection points which are not marked). Sub-synchronous frequency AB appears before the speed soaring point B (14519 rpm), and this accumulates energy for speed soaring process. The ratio of speed to turbine flow is nearly linear according to the impeller characteristic. The proportion coefficient is about 109 (rpm)/(Nm³/h) at the regions without low frequency vibration. The proportion coefficient is about 17.7 (rpm)/(Nm³/h) during the AB region, which is far less than the normal coefficient value (109 (rpm)/(Nm³/h)) in the flow range from 100 Nm³/h to 290 Nm³/h as shown in Fig. 3. That is because sub-synchronous frequency vibration occurs in the AB region which accumulates energy.

The BC region is the speed-soaring process where the speed increases from 14626 rpm to 39465 rpm quickly with the flow increasing from 290 Nm³/h to 368 Nm³/h respectively, and the ratio of speed to turbine flow is 318 (rpm)/(Nm³/h), far greater than the normal coefficient value (109 (rpm)/(Nm³/h)). This is because sub-synchronous frequency vibration disappears at the point B where the accumulating energy of sub-synchronous frequency is delivered to the normal frequency vibration. In the first half of the speed-soaring process, the amplitude of the vibration is smaller relatively, and the speed-soaring rate is higher. The amplitude of the vibration is higher in the latter half of the speed-soaring process than the first half and the rising rate decreases. So the amplitude of the vibration should be controlled to prevent rubbing.

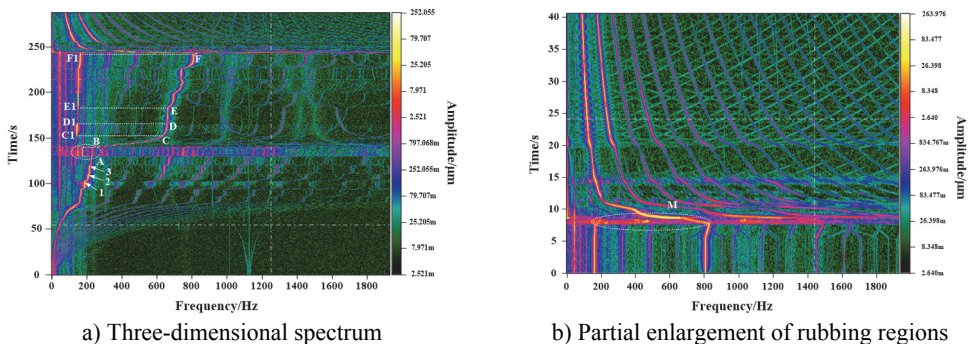


Fig. 2. Three-dimensional spectrums for speed-up and speed-down process at vertical direction of turbine end

At the speed of 37693 rpm, gas whip appears and the frequency of gas whip is 141 Hz. The gas whip of CD region disappears at the speed of 39423 rpm.

When the speed goes up to 39712 rpm, the gas whip appears again. Its whip frequency is 147 Hz and increases slightly with the speed. The whip frequency increases to 152 Hz, and the corresponding power frequency speed increasing to 44711 rpm.

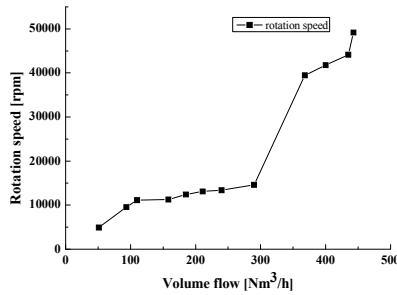


Fig. 3. Rotation speed changes with volume flow

3.2.1. Analysis for the effect of bearing gas supply pressure on gas film whipping

Point D is the vanishing point of low frequency in CD section. At the point D, the bearing gas supply pressure of the turbine and compressor end is changed, which is helpful to delay the low frequency and improve the stable speed range. The influence of bearing gas supply pressure on the dynamical characteristics in the CF section will be discussed in detail.

3.2.1.1. Analysis of nonlinear dynamical behaviors in the CF section

The bifurcation for the repeated appearance and disappearance of the low frequency whip is given in Fig. 4. The gas film whip frequency which occurred at the speed of 37693 rpm is 141 Hz, as shown in Fig. 5(a). At this time, the amplitude of the gas whip is smaller and the orbit of shaft center is period one. During the speed range of 37693 rpm to 39200 rpm, the frequency of the gas film whip is unchanged with the increasing speed. The amplitude of gas film whip increases with the speed, as shown in Fig. 5(b) to 5(d).

At the speed of 39000 rpm, the supply pressure of gas bearing increases from 0.65 MPa to 0.8 MPa. The vibrational amplitude at the speed of 39200 rpm shows a trend of convergence owing to the change of bearing gas supply pressure. The 200 rpm speed difference is caused by the delay of the control system and the valve. The gas film whip disappears at the point D, and the amplitude is controlled within 3 μm, as shown in Fig. 5(e). When the speed increases to 39712 rpm, gas film whip appears again and the whip frequency is 147 Hz, as shown in Fig. 5(f). The corresponding vibrational amplitude of gas film whip increases with the rotate speed. At the speed of 41500 rpm, the amplitude of the low frequency vibration is controlled within 30 μm, as shown in Fig. 5(g). The boundary of the direct frequency vibration isn't divergent from 41500 rpm to 44500 rpm (see Fig. 4), and the orbit of shaft center presents quasi periodic motion during the speed range.

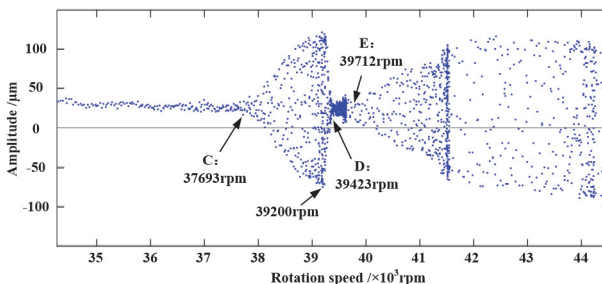


Fig. 4. Bifurcation of CF region

The direct frequency vibration amplitude can be controlled within the safety threshold and not increase with the speed after taking an appropriate bearing gas supply pressure plan. The bearing-rotor system can be thought to be stable during the CF region.

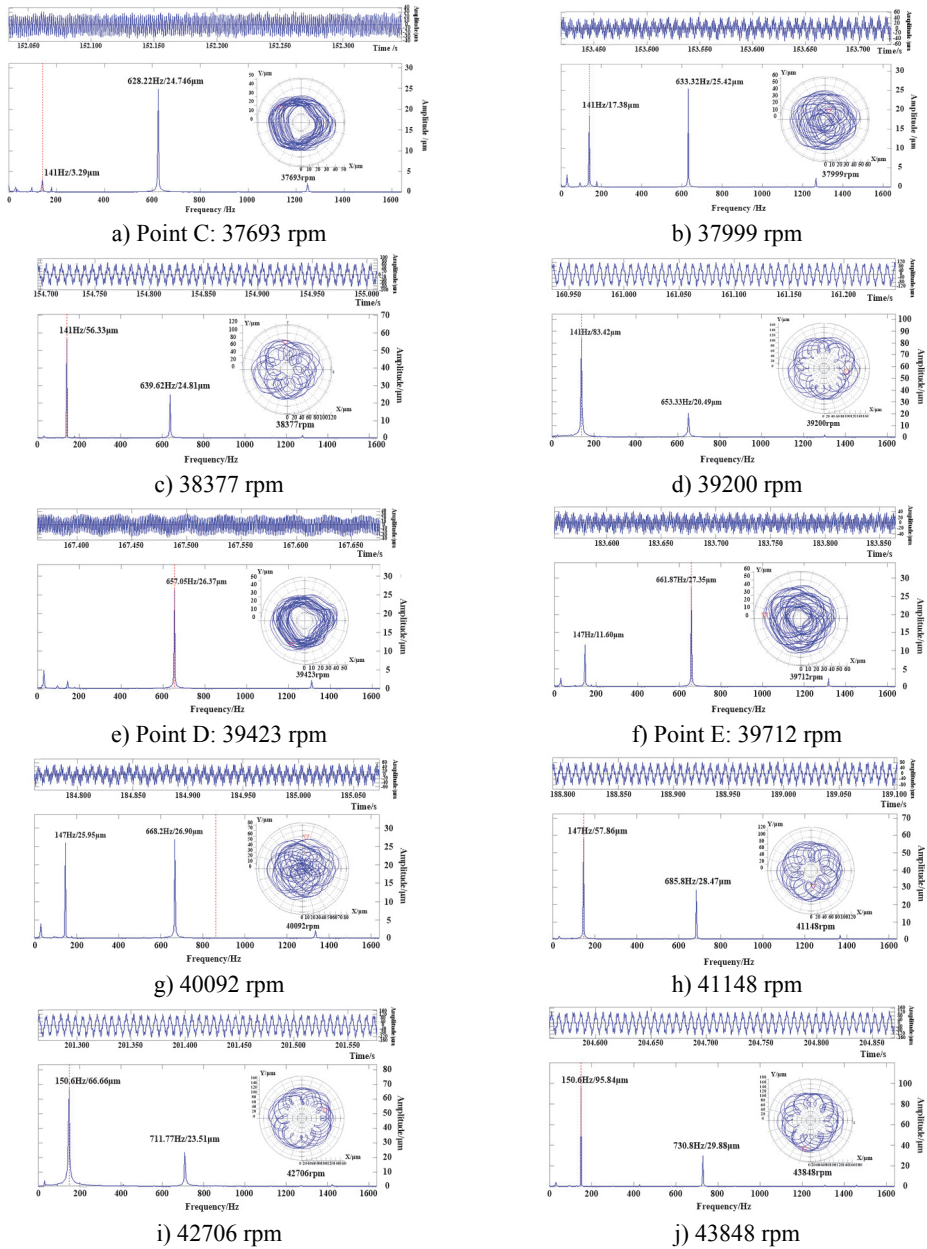


Fig. 5. Spectral analysis maps and the orbits of shaft center for CF region

3.2.2. Characteristic analysis for gas film whipping

Without considering gas film damping of bearing, the change characteristics with different bearing gas supply pressure are given according to the modal test [12]. At the pressure of 0.65 MPa, the gas film stiffness is about 3.00×10^6 N/m. Combining the corresponding numerical simulation results, the first order critical feature is conical whirling motion at 8255 rpm (137.6 Hz). The second order critical feature is cylindrical whirling motion at 14246 rpm (237.4 Hz).

Based on the nonlinear analysis of CF section in Fig. 4, the locking frequency of gas film whip is 141 Hz at the speed of 37693 rpm. The locking frequency increases to 150 Hz when the rotate

speed is at 43800 rpm. The locking frequency of gas film whip is around the first critical speed by the comparative analysis, slightly above the first critical speed with the increasing speed. That is due to dynamic characteristic of gas film.

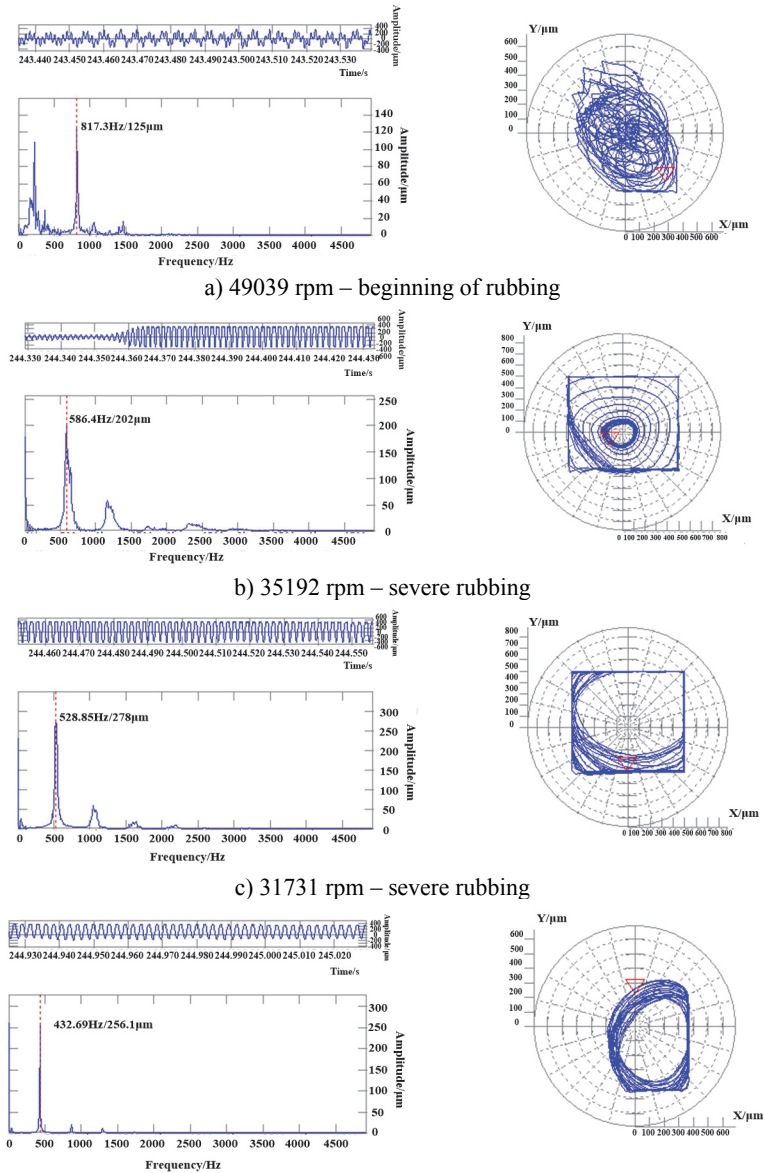


Fig. 6. Dynamic characteristics of the rubbing process

3.2.3. Characteristic analysis for rubbing

Rubbing occurs at the speed of 49039 rpm during the speed-down process. The continuous spectrum feature including low and high frequency is presented in Fig. 6(a). The rubbing characteristics can be obtained from the orbits of shaft center at 49039 rpm. The rotor goes into the severe rubbing areas from 35000 rpm to 31000 rpm. At the same time, the power frequency vibration is above 500 μm, and the peak clipping phenomenon happens in the time domain

waveform. The orbits of shaft center show square features during the region. The spectrum features and orbits of the rotor backing out of the rubbing area are given in Fig. 6(d). The power frequency vibration is major at 25961 rpm.

Because of the large power frequency amplitude, the rubbing fault in the speed-down experiment occurs. It's necessary to improve rotor dynamic balancing precision at the high speed for eliminating rubbing fault owing to power frequency vibration.

4. Conclusions

Experimental research on dynamic characteristics of gas bearing-rotor system with the coaxial multi discs are studied, the main conclusions are described as follows.

Gas film whipping occurs at the region of high speed in the gas bearing-rotor system. The locking frequency of gas film whipping is at the lowest order natural frequency of shafting.

The reasonable bearing gas supply pressure plans can postpone the beginning rotational speed of gas film whipping, and control the boundary of the vibrations. The shafting stability is improved under reasonable bearing gas supply pressure plans.

At the beginning of the rubbing, continuous maps including high frequencies and low frequencies are presented in the spectral analysis maps. In the severe rubbing stage, the apparent peak clipping feature appears at the maps of time do-main waveform, and the corresponding axis center tracks are from oval to square. The typical spectrums provide an effective support for identify and diagnosis of the corresponding fault.

References

- [1] **Li S., Guo Y., Zhu Z., et al.** Static characteristics analysis and basic parameters optimization of aerostatic bearing for precision machine tool. *Lubrication Engineering*, Vol. 37, 2012, p. 29-32, (in Chinese).
- [2] **Ren J.** Air refrigerator. *Refrigeration and Air Conditioning*, Vol. 8, 2008, p. 15-21, (in Chinese).
- [3] The State Council of the People's Republic of China. *National Medium and Long-Term Science and Technology Development Plan (2006-2020)*. Beijing, 2006, (in Chinese).
- [4] **Liu D.** American advanced microturbine planning. *Energy Research and Information*, Vol. 1, 2002, p. 59-60, (in Chinese).
- [5] **San Andrés L., Ryu K.** Hybrid gas bearings with controlled supply pressure to eliminate rotor vibrations while crossing system critical speeds. *Journal of Engineering for Gas Turbines and Power*, Vol. 130, 2008, p. 062505-1-062505-10.
- [6] **Morosi S., Santos I. F.** On the modelling of hybrid aerostatic-gas journal bearings. *Proceedings of the Institution of Mechanical Engineers, Part J: Journal of Engineering Tribology*, Vol. 225, 2011, p. 641-653.
- [7] **Morosi S., Santos I. F.** Active lubrication applied to radial gas journal bearings. Part 1: Modeling. *Tribology International*, Vol. 44, 2011, p. 1949-1958.
- [8] **Chen C., Guo Y., Ye S.** The Experimental study of an air bearing medium-pressure expansion turbine. *Journal of Refrigeration*, Vol. 4, 1982, (in Chinese).
- [9] **Yang J.** Study on Stability of Fluid Dynamic Lubricates and Bearing Rotor System. North China Electric Power University, China, Beijing, 2006, (in Chinese).
- [10] **Yang J., Chen C., Yang S., et al.** An analytic model of oil-film force on hydrodynamic journal bearing of finite length. *Proceedings of GT2009, ASME Turbo Expo: Power for Land, Sea, and Air*, Berlin, Germany, 2008.
- [11] **Chen Ce** Research on Rotor-bearings System Nonlinear Dynamic Dynamics Behaviors, Fluid-solid Interaction and Its Frequency Modulations. Institute of Engineering Thermophysics, Chinese Academy of Sciences, China, Beijing, 2008, (in Chinese).
- [12] **Han D.** Stability Analysis and Experimental Investigation on High-speed Turbomachinery Shafts. Institute of Engineering Thermophysics, Chinese Academy of Sciences, China, Beijing, 2014, (in Chinese).